

See discussions, stats, and author profiles for this publication at: <http://www.researchgate.net/publication/51295687>

Functional connectivity in the motor cortex resting human brain using echo-planar MRI

ARTICLE *in* MAGNETIC RESONANCE IN MEDICINE · OCTOBER 1995

Impact Factor: 3.57 · Source: PubMed

CITATIONS

2,702

READS

2,991

4 AUTHORS, INCLUDING:



Bharat Biswal

New Jersey Institute of Technology

200 PUBLICATIONS 14,364 CITATIONS

SEE PROFILE



Victor M Haughton

University of Wisconsin-Madison

473 PUBLICATIONS 17,284 CITATIONS

SEE PROFILE

Functional Connectivity in the Motor Cortex of Resting Human Brain Using Echo-Planar MRI

Bharat Biswal, F. Zerrin Yetkin, Victor M. Haughton, James S. Hyde

An MRI time course of 512 echo-planar images (EPI) in resting human brain obtained every 250 ms reveals fluctuations in signal intensity in each pixel that have a physiologic origin. Regions of the sensorimotor cortex that were activated secondary to hand movement were identified using functional MRI methodology (fMRI). Time courses of low frequency (<0.1 Hz) fluctuations in resting brain were observed to have a high degree of temporal correlation ($P < 10^{-3}$) within these regions and also with time courses in several other regions that can be associated with motor function. It is concluded that correlation of low frequency fluctuations, which may arise from fluctuations in blood oxygenation or flow, is a manifestation of functional connectivity of the brain.

Key words: functional connectivity; motor cortex; fMRI; EPI.

INTRODUCTION

Physiological fluctuations in resting brain have been observed by several groups using echo-planar magnetic resonance imaging (EPI, MRI) (1–4). These fluctuations are apparent in a time course of signal intensities from a given pixel as a function of image number (i.e., “time”). A Fourier transform of a typical time course shows peaks at the heart and respiratory frequencies. Peaks are also seen at harmonics of the heart rate and as respiratory sidebands symmetrically disposed about the fundamental heart frequency. In addition, poorly characterized low-frequency fluctuations (<0.1 Hz) are observed. This communication concerns these low-frequency fluctuations. We have discovered that low-frequency fluctuations in resting brain from regions of the primary sensory motor cortex that are associated with hand movement are strongly correlated both within and across hemispheres.

Correlations of electrical activity in the rat cerebral cortex with previously unrecognized spontaneous fluctuations in regional cerebral blood flow (rCBF) have been recently reported (5). The characteristic frequency of these fluctuations is about the same as the fluctuations in human brain described in the present communication. It has been established in the context of human fMRI investigations that task-induced neuronal activity is correlated with changes in both rCBF and blood oxygenation. The apparatus used in the present study has been opti-

mized for sensitivity to blood oxygenation, although flow sensitivity remains, and it seems likely that fluctuations in both cortical blood oxygenation and flow are being observed. It is suggested that the fluctuations observed in the rat (5) and by us in humans are of a similar nature, noting that fluctuations in rCBF are accompanied by fluctuations in blood oxygenation. Cortical oscillations have been reported by a number of investigators, and ref. 5 provides access to that literature.

MATERIALS AND METHODS

Eleven healthy human volunteers self-identified as right handed (eight male and three female, between the ages of 24 and 37 years) with no history of head trauma or neurological disease, no current use of medication and no contraindication to MRI were scanned (6). Five of these subjects were recruited by a colleague working on a different project. They were unknown to us and to the best of our knowledge had not previously participated in medical research. The remaining subjects were students working in unrelated fields and with minimal knowledge of MRI. A standard GE 1.5 T Signa clinical scanner equipped with a home-built three-axis balanced-torque head gradient coil and a shielded end-capped quadrature transmit/receive birdcage radio frequency coil was used (6, 7). For imaging, the volunteers were positioned supine on the gantry of the scanner with the head in a midline location in the coil. Foam padding was used to limit head movement. A single axial slice across the motor cortex (8) was obtained from each volunteer.

Imaging began with the acquisition of high resolution axial images using a GRASS pulse sequence, with $TR = 600$ ms, $TE = 10$ ms, $FOV = 24$ cm, and a matrix size = 256×256 . For functional imaging, several time series of 512 EPI images were obtained using a single axial slice with a GE EPI sequence, a FOV of 24 cm, a matrix size of 64×64 , a slice thickness of 10 mm, (corresponding to a spatial resolution of $3.75 \times 3.75 \times 10$ mm), and a TE of 40 ms. In four volunteers, time course images were acquired with a TR of 250 ms, and a flip angle of 34° . A TR value of 500 ms (flip angle of 67°) was used in two studies and a TR of 1000 ms (flip angle of 81°) in the others.

During the resting state acquisitions, the subjects were instructed to refrain from any cognitive, language, or motor tasks as much as possible. Four subjects were told of the sequence of scans to be done, i.e., first scan would be rest, second would be finger tapping. To minimize the possibility of imagining finger tapping, seven subjects were scanned after being told the wrong tasks. In one study, time-course images were obtained from the motor cortex while the subject was shown a visual stimulus (9). After the visual stimulus, the subject was instructed to

MRM 34:537–541 (1995)

From the Biophysics Research Institute and Department of Radiology (F.Z.Y., V.M.H.), Medical College of Wisconsin, Milwaukee, Wisconsin.

Address correspondence to: James S. Hyde, Ph.D., Biophysics Research Institute, Medical College of Wisconsin, PO Box 26509, 8701 Watertown Plank Rd., Milwaukee, WI 53226-0509.

Received February 15, 1995; revised June 22, 1995; accepted June 27, 1995.

The work was supported by grant CA41464 from the National Institutes of Health (to JSH).

0740-3194/95 \$3.00

Copyright © 1995 by Williams & Wilkins

All rights of reproduction in any form reserved.

perform bilateral finger tapping. In six other studies, subjects were told that the activation was an auditory stimulus. After the resting and auditory time-course images were obtained along the motor cortex, they were then asked to perform motor tasks. These seven subjects had not previously been given any indication that a motor task would eventually be requested.

For task activation, bilateral finger tapping was used. Subjects were asked to tap each finger to the thumb sequentially at a self-paced rate without moving their arms. A time course of single shot gradient-recalled EPI consisted of 20-s periods at rest alternating with 20 s of motor tasks.

For mapping of motor function, a square wave reference with 20-s periods of "task activation" assigned a value of 1 alternating with 20-s periods of "rest" assigned a value of 0 was used. All time course pixels from the functional image were normalized between 0 and 1 and cross-correlated with the ideal square wave (10). After applying the Bonferroni correction, a threshold corresponding to statistical significance value $P < 0.001$ was calculated. All pixels that passed the threshold were identified as belonging to the finger motor cortex. Pixels in the left and right motor cortices that were activated by the finger task were identified (10, 11). There were approximately 60 such pixels in each study. About 1000 of the possible 4096 pixels (i.e., 64×64) were in brain tissue. A finite impulse-response low-pass filter (12) with a cut-off frequency of 0.08 Hz was then applied to all time courses in the EPI data set of resting brain (13). Each of the resting brain time courses from the regions that had been identified by fMRI was used as a reference to produce, from each resting brain study, approximately 60 correlation-coefficient images (10). Pixels in each of these images that passed the correlation-coefficient of 0.35, which corresponds to a significance value of $P < 10^{-3}$, were counted.

RESULTS

Figure 1a shows a representative filtered time course from a pixel that was identified as lying within the finger-hand motor cortex, and Fig. 1b shows a portion of the Fourier transform. The magnitude of the signal in Fig. 1a, which is from grey matter, is 465 (arbitrary units). Typical fMRI signal intensities in motor cortex are 4% of this value, and the rms value of the fluctuations is 0.5 to 1%. Low-frequency fluctuations in white matter are reduced relative to grey matter by about 60%, and have not been studied in detail. Fluctuations in all grey matter regions are qualitatively similar. The significance of the peaks seen in Fig. 1b has not yet been investigated.

Pixel-counting results are tabulated in Table 1. Brain tissue in the axial slice was divided into three regions, designated L , R , and O , containing n_L , n_R , and n_O pixels, respectively. Here L and R refer to the left and right motor cortices as determined by fMRI and O to all other brain tissue. As an example of the counting procedure, consider the column of Table 1 labeled \bar{n}_{LR}/n_L . The average number of pixels passing the threshold in region L is found using as a reference, one-by-one, the time course of each pixel in region R . For each of these n_R reference time

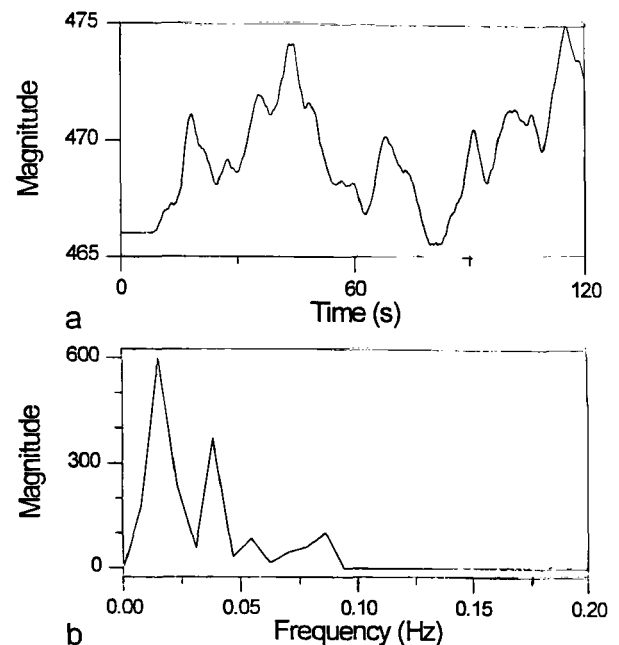


FIG. 1. (a) Representative time course of motor cortex physiological fluctuations after FIR filtering that passes frequencies < 0.08 Hz. (b) Fourier transform of the time course.

courses, some number of pixels is counted and the average number of counted pixels, \bar{n}_{LR} is determined. Data are expressed as $(\bar{n}_{LR}/n_L) \times 100$ (percent). Pairwise correlations have been determined in this procedure, which produces a subset of the entries in the sample correlation matrix. This matrix has a dimensionality of about 1000×1000 since there are about 1000 pixels in the plane of section using the protocol of this report.

Correlations within a region are labeled \bar{n}_{RR}/n_R , \bar{n}_{LL}/n_L and correlations between regions by \bar{n}_{LR}/n_L , which is necessarily identical to \bar{n}_{RL}/n_R . The quantity $(\bar{n}_{OL} + \bar{n}_{OR})/n_O$ serves as a control. This is the average number of pixels in "other" brain tissue that passes the threshold when using a motor cortex time course as a reference. As a specific numeric example, when using left motor cortex references about 20 of the 30 pixels in right motor cortex and about 20 of the 1000 pixels in "other" brain tissue are counted.

Without exception for the 11 subjects, $\bar{n}_{LL}/n_L > \bar{n}_{RR}/n_R > \bar{n}_{LR}/n_L$, although the differences for a given subject are not significant. The mean value of percentages for each subject are the same within statistical uncertainty. We interpret \bar{n}_{LR}/n_L as a measure of connectivity of motor cortex function across hemispheres.

The possibility of contribution of system noise or system instability to the correlation was studied using a phantom under identical imaging parameters. Using the same significance value, no pixels, other than the reference, passed the threshold. Even for a low threshold value of 0.1, which corresponds to a statistically insignificant P value, no pixels, other than the reference, passed the threshold.

No significantly different statistics were observed in Table 1 for the three different TRs (250, 500, and 1000 ms). TRs of 250, 500, and 1000 ms correspond to fre-

Table 1
Correlation Coefficient Data from Resting Brain

| Subject | TR (ms) | \bar{n}_{LL}/n_L % | \bar{n}_{LR}/n_L % | \bar{n}_{RR}/n_R % | Mean | $(\bar{n}_{OL} + \bar{n}_{OR})/n_O$ % |
|---------|---------|----------------------|----------------------|----------------------|---------|---------------------------------------|
| 1 | 250 | 88 ± 8 | 65 ± 11 | 74 ± 9 | 73 ± 10 | 1.8 |
| 2 | 250 | 84 ± 9 | 63 ± 13 | 75 ± 10 | 71 ± 11 | 2.2 |
| 3 | 250 | 93 ± 5 | 77 ± 12 | 85 ± 9 | 83 ± 12 | 2.4 |
| 4 | 250 | 83 ± 11 | 66 ± 17 | 74 ± 12 | 72 ± 15 | 1.6 |
| 5 | 500 | 71 ± 14 | 56 ± 19 | 62 ± 9 | 61 ± 16 | 1.7 |
| 6 | 400 | 79 ± 12 | 61 ± 17 | 67 ± 14 | 67 ± 15 | 0.9 |
| 7 | 1000 | 79 ± 9 | 67 ± 13 | 74 ± 10 | 72 ± 11 | 1.6 |
| 8 | 1000 | 73 ± 7 | 53 ± 9 | 70 ± 8 | 65 ± 8 | 3.5 |
| 9 | 1000 | 69 ± 11 | 42 ± 9 | 71 ± 12 | 60 ± 11 | 1.9 |
| 10 | 1000 | 82 ± 9 | 69 ± 10 | 79 ± 8 | 76 ± 9 | 3.5 |
| 11 | 1000 | 77 ± 9 | 59 ± 12 | 65 ± 11 | 67 ± 11 | 4.3 |

quency bandwidths of 2, 1, and 0.5 Hz. Due to hardware limitations, we were able to acquire only 512 images per scan, irrespective of the TR. For TR of 250 ms with a total span of 120 s, the respiratory and cardiac rates were filtered using the FIR filter. For TRs of 500 and 1000 ms, total temporal spans of 240 and 480 s of data were acquired with some aliasing due to the cardiac rate. Although studies with TR = 250 ms demonstrate that the spatial correlation is due to some low uncharacterized frequencies and not due to respiratory or cardiac rates, similar results with TR = 500 and 1000 ms demonstrate that these low frequencies are present at all times and that aliasing is not a major problem.

Figure 2 shows histograms of the distribution of correlation coefficient magnitudes. Regions L and R were defined as for Table 1. The histogram labeled “Rest Opposite” contains all n_{LR} and n_{RL} entries in the correlation coefficient matrix from resting brain for all seven subjects. A normalized distribution was obtained for each subject. Figure 2 shows the mean distribution across the eleven subjects. Similarly, “Rest Same side” contains all n_{RR} and n_{LL} entries. This same procedure was repeated for task-activation data.

Although the resting data appear somewhat similar to the task-activated data, this is because correlation coefficient magnitudes rather than cross-correlation magnitudes are shown. The correlation coefficient is a measure of the similarity of shapes of two waveforms, but not of their relative amplitudes.

One notes more strongly correlated pixel pairs in the task-activated data than the resting brain data, but a few strongly correlated pixel pairs are seen in the latter. A model of random noise treated in this same statistical way shows that less than 1% of pixel pairs have correlation coefficients above 0.35. Such a model also peaks at 0, in contrast to the experimental data of Fig. 2.

Figure 3a shows an FMRI response from bilateral finger movement (Subject 1) overlaid on an anatomic image, and Fig. 3b shows a corresponding image produced using methods described in this report. Namely, a central pixel in the left motor cortex (region b of Fig. 3b) was identified. The filtered time course from this pixel served as a reference in determining the correlation coefficient with all other filtered time courses, and those pixels with correlation coefficient >0.35 ($P < 10^{-3}$) were colored, as shown in Fig. 3b. About 10% of the colored pixels in

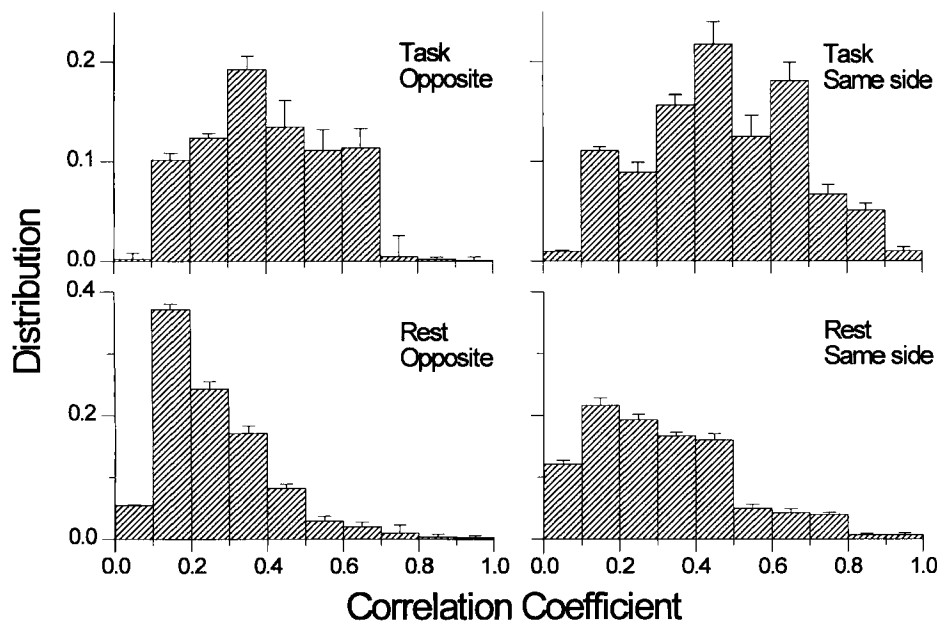


FIG. 2. Normalized distribution of magnitudes of correlation coefficients for all entries in regions L and R of the correlation-coefficient matrix for two experiments: resting (lower) and task activation (upper). Pixel pairs for opposite sides are at the left and for the same side at the right.

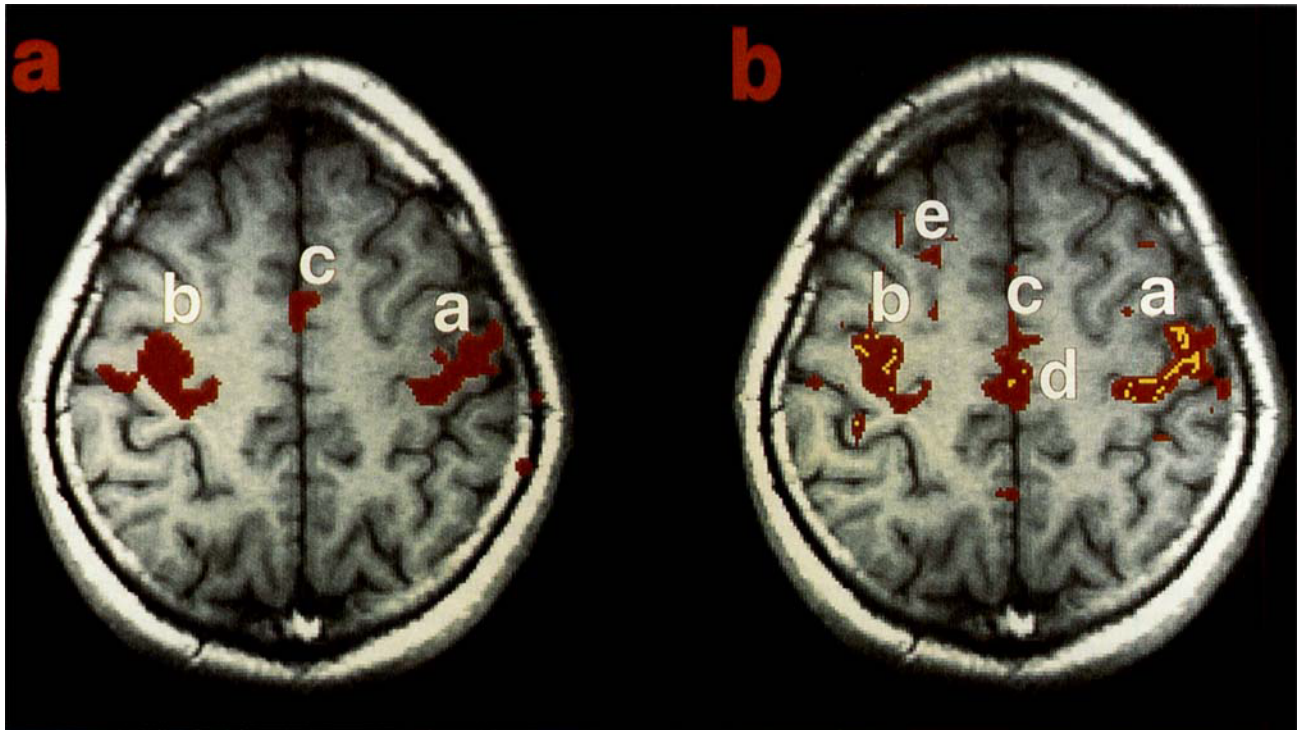


FIG. 3. (Left) FMRI task-activation response to bilateral left and right finger movement, superimposed on a GRASS anatomic image. (Right) Fluctuation response using the methods of this paper. See text for assignment of labeled regions. Red is positive correlation, and yellow is negative.

Fig. 3b are negative rather than positive correlations. Details of this observation are not understood. Negative correlations are occasionally encountered in *task-induced* FMRI at the outer boundary of the brain because of head motion. No negative correlations of this type were observed in the present study from *resting brain*.

Several observations can be made concerning Fig. 3. Table 1 shows that \bar{n}_{LR}/n_L is 65% for Subject 1, but areas of the colorized regions of right and left motor cortex (labeled *a*, *b*) are about the same in both Figs. 3a and 3b. This apparent discrepancy is because 5 or 6 pixels in region *a* of Fig. 3b lay outside the right motor cortex boundary as determined by FMRI (i.e., region *a* of Fig. 3a), but were contiguous to it. There are no “holes” surrounded by colorized pixels in either the left or right motor cortex. A few pixels are seen in both images on midline in region *c* that can be assigned to Broadman’s area 6. This region, which is more pronounced in Fig. 3a than in Fig. 3b, can probably be assigned to the supplementary motor area (SMA) (11). Pixels posterior to region *c*, labeled *d*, were identified as belonging to the paracentral lobule. Region *d* may be an extension of the primary sensorimotor cortex into the inner hemispheric fissure. The activated area in Fig. 3b labeled *e*, which is also seen occasionally in motor-task FMRI data (13) although not in this case in Fig. 3a, may represent the premotor area. Many of the colorized pixels that were not coincident with the motor cortex areas as defined by FMRI seem nevertheless to be a manifestation of functional connectivity.

CONCLUSION

Similar fluctuations giving rise to functional connectivity have been observed by us in the auditory and visual cortex. We believe that the functional connectivities demonstrated in the motor cortex are a general phenomena and not due to “imagined” motor tasks. Previous studies on imagined motor tasks (11, 13) reported activation in the SMA but not in the primary motor cortex, in contrast to our results. Further, imagined activation would be expected to be random for each subject as well as between subjects.

Bandettini *et al.* (10) discuss three methods for obtaining the reference vector in order to determine the correlation coefficient and cross correlation magnitude: a) use of a simple box-car waveform shifted by the hemodynamic response, as in the present study, b) use of the experimental time course in a selected activated pixel, and c) development of a time-averaged response vector. An immediate concern arises about the use of methods b) and c) because of the existence of correlation within and between functionally related regions during rest. The correlation coefficient cc can be written

$$cc = \frac{\sigma_f \cdot \sigma_r}{\sigma_f \sigma_r},$$

where σ_r is the reference vector and σ_f is the experimental vector including response that is time locked to the task as well as physiological fluctuations and system noise. If physiological fluctuations contribute not only to σ_f , but also to σ_r , as in method b) and c), and if these

fluctuations are correlated as discussed here, the value of cc will be increased relative to use of a boxcar or other synthesized waveform. Comparison of results using different reference vectors may present an opportunity for more detailed investigation of fMRI response.

Correlation of fluctuations across the entire brain using a whole-volume RF head coil as described here is obviously desirable, but improved data quality can be obtained in restricted superficial regions of cortex using surface coils. A recommended direction for future research on brain fluctuations would be the use of both whole volume and surface coils in concert.

Concepts of anatomical, functional, and effective connectivity have been developed in recent years in a context of electrophysiology (14, 15) and positron emission tomography (16). Functional connectivity was defined in ref. 16 as the temporal correlation of a neurophysiological index measured in different brain areas. This report demonstrates that functionally related brain regions exhibit correlation of low frequency fluctuations in the resting state as detected by echo-planar MRI. It is concluded that low frequency fluctuation of blood flow and oxygenation is indeed a neurophysiological index.

ACKNOWLEDGMENTS

The authors thank E. A. DeYoe for advice on the paradigms used for task-induced fMRI studies and R. W. Cox for advice on mathematics.

REFERENCES

1. B. Biswal, P. A. Bandettini, A. Jesmanowicz, J. S. Hyde, Time-frequency analysis of functional EPI time-course series, in "Proc., SMRM, 12th Annual Meeting, New York, 1992," p. 722.
2. P. Jezzard, D. LeBihan, D. Cuenod, L. Pannier, A. Prinster, R. Turner, An investigation of the contribution of physiological noise in human functional MRI studies at 1.5 tesla and 4 tesla, in "Proc., SMRM, 12th Annual Meeting, New York, 1992," p. 1392.
3. R. M. Weisskoff, J. Baker, J. Belliveau, T. L. Davis, K. K. Kwong, M. S. Cohen, B. R. Rosen, Power spectrum analysis of functionally-weighted MR data: what's in the noise? in "Proc., SMRM, 12th Annual Meeting, New York, 1992," p. 7.
4. B. Biswal, E. A. DeYoe, A. Jesmanowicz, J. S. Hyde, Removal of physiological fluctuations from functional MRI signals, in "Proc., SMR, 2nd Annual Meeting, San Francisco, 1994," p. 653.
5. E. V. Golanov, S. Yamamoto, D. J. Reis, Spontaneous waves of cerebral blood flow associated with patterns of electrocortical activity. *Am. J. Physiol.* **266**, R204–214 (1994).
6. E. C. Wong, P. A. Bandettini, J. S. Hyde, Echo-planar imaging of the human brain using a three axis local gradient coil, in "Proc., SMRM, 11th Annual Meeting, SMRM, Berlin, 1992," p. 105.
7. E. C. Wong, E. Boskamp, J. S. Hyde, A volume optimized quadrature elliptical endcap birdcage brain coil, in "Proc., SMRM, 11th Annual Meeting, Berlin, 1992," p. 4014.
8. C. Rumeau, N. Tzouri, N. Murayama, P. Peretti-Viton, G. Salomon, Location of hand function in the sensorimotor cortex: MR and functional correlations. *AJNR* **15**, 567 (1994).
9. E. A. DeYoe, J. Neitz, P. A. Bandettini, E. C. Wong, J. S. Hyde, Time course of event-related MR signal enhancement in visual and motor cortex, in "Proc., SMRM, 12th Annual Meeting, New York, 1992," p. 1824.
10. P. A. Bandettini, A. Jesmanowicz, E. C. Wong, J. S. Hyde, Processing strategies for time-course data sets in functional MRI of the human brain. *Magn. Reson. Med.* **30**, 161 (1993).
11. P. E. Roland, B. Larsen, N. A. Lassen, E. Skinhøj, Supplementary motor areas and other cortical areas in organization of voluntary muscle movements in man. *J. Neurophysiol.* **43**, 118 (1980).
12. R. W. Hamming, in "Digital Filters," 2nd ed., Prentice Hall, Englewood Cliffs, NJ, 1983.
13. S. M. Rao, J. R. Binder, P. A. Bandettini, T. A. Hammeke, F. Z. Yetkin, A. Jesmanowicz, L. M. Lisk, G. L. Morris, W. M. Mueller, L. D. Estkowski, E. C. Wong, V. M. Haughton, J. S. Hyde, Functional magnetic resonance imaging of complex human movements. *Neurology* **43**, 2311 (1993).
14. G. L. Gerstein, P. Bedenbaugh, A. M. H. J. Aertsen, Neuronal assemblies. *IEEE Trans. Biomed Eng.* **36**, 4 (1989).
15. P. M. Gochin, E. K. Miller, C. G. Gross, G. L. Gerstein, Functional interactions among neurons in inferior temporal cortex of the awake macaque. *Brain Res.* **84**, 505 (1991).
16. K. J. Friston, C. D. Frith, P. F. Liddle, R. S. J. Frackowiak, Functional connectivity: the principle-component analysis of large (PET) data sets. *J. Cerebral Blood Flow Metab.* **13**, 5 (1993).